

Resonances and wave propagation velocity in the subglottal airways

Steven M. Lulich^{a)}

Department of Psychology Washington University Saint Louis MO 63130

Abeer Alwan and Harish Arsikere

Department of Electrical Engineering UCLA Los Angeles CA 90095

John R. Morton and Mitchell S. Sommers

Department of Psychology Washington University Saint Louis MO 63130

(Dated: August 12, 2011)

Previous studies of subglottal resonances have reported findings based on relatively few subjects, and the relations between these resonances, subglottal anatomy, and models of subglottal acoustics are not well understood. In this study, accelerometer signals of subglottal acoustics recorded during sustained [a:] vowels of 50 adult native speakers (25 males, 25 females) of American English were analyzed. The study confirms that a simple uniform tube model of subglottal airways, closed at the glottis and open at the inferior end, is appropriate for describing subglottal resonances. The main findings of the study are: 1) whereas the walls may be considered rigid in the frequency range of Sg2 and Sg3, they are yielding and resonant in the frequency range of Sg1, with a resulting $\sim 4/3$ increase in wave propagation velocity and, consequently, in the frequency of Sg1; 2) the ‘acoustic length’ of the equivalent uniform tube varies between 18 cm and 23.5 cm, and is approximately equal to the height of the speaker divided by an empirically determined scaling factor; 3) trachea length can also be predicted by dividing height by another empirically determined scaling factor; and 4) differences between the subglottal resonances of males and females can be accounted for by height-related differences.

PACS numbers: 43.70.Bk, 43.70.Aj, 43.20.Hq

I. INTRODUCTION

Since van den Berg’s seminal study of the acoustic properties of the subglottal airways²⁹, it has been observed^{15,16} that the frequencies of the second and third subglottal resonances (Sg2 and Sg3, respectively) are nearly odd integer multiples of the frequency of the first subglottal resonance (Sg1). Nearly, but not quite: the ratio of Sg2/Sg1 is somewhat smaller than 3, and likewise the ratio of Sg3/Sg1 is somewhat smaller than 5, although the ratio of Sg3/Sg2 is very close to the expected value of 5/3, on the average (as will be shown in Section III.A).

The subglottal system is comprised of a branching tree network of airways. The inferior end of the trachea bifurcates into two primary bronchi, which also bifurcate into small airways, and so on up to approximately 35 bifurcations^{11,31}. These bifurcations are generally asymmetrical, with one daughter airway being somewhat larger than its sister airway, and in fact strict bifurcation of airways into two (and only two) daughter airways is not always observed^{13,31}. This complex branching airway tree is frequently modeled using simpler structures, including symmetrical branching trees^{11,12,21,31}, and equivalent non-branching tubes with variable cross-sectional area as a function of distance inferiorly from the glottis^{15,29,32}. Perhaps the simplest model of the subglottal airways is as a uniform tube with rigid walls,

closed at the glottis and open at the inferior end, with a length close to 20 cm. Such a model predicts Sg2 and Sg3 well, but predicts a lower frequency for Sg1 than is found empirically. Anatomically, the area function of the subglottal airways (in which the cross-sectional areas of each airway at a given distance from the glottis are summed together) is roughly uniform between the glottis and approximately 20 cm inferior to the glottis (after about 4 bifurcations), and expands very quickly (faster than exponential) beyond this point¹⁵ (see Figure 1), so that the simple uniform tube model seems appropriate, except for the fact that the subglottal airways do not have rigid walls.

Van den Berg²⁹ attributed the deviation of Sg1 from its predicted frequency to the shape of the expanding area function beyond 20 cm, which according to his model reaches a plateau between 24 cm and 26 cm from the glottis before resuming its greater than exponential increase. He also noted that the speed of sound (more appropriately the phase or wave propagation velocity, measured with a 300 Hz tone) appeared to be significantly lower in the subglottal airways than in the free-field, and this he attributed to the compliance of the airway walls, analogous to the effect of arterial wall compliance on the pulse wave velocity given by the Moens-Korteweg equation²⁵. Ishizaka *et al.*¹⁵ attributed the deviation of Sg1 directly to the airway wall impedance, although they claimed that the airway walls are inertive rather than compliant. In their simulations, a rigid-walled model of the lower airways led to a frequency of Sg1 as low as 3/5 times the measured frequency, whereas a soft-walled model led to Sg1 frequencies closer to measured values.

^{a)}Electronic address: slulich@wustl.edu

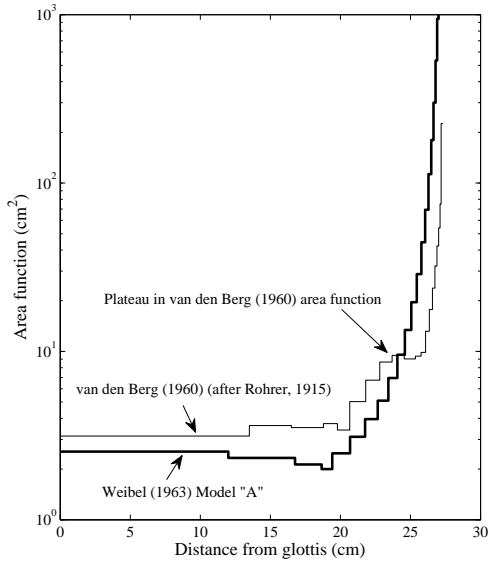


FIG. 1. Area functions of the subglottal airways from the glottis inferiorly into the tracheobronchial tree, based on the models of Weibel³¹ and van den Berg²⁹. The model of van den Berg is based on anatomical data reported by Rohrer²⁶. In both models, the cross-sectional area is roughly constant for approximately 20 cm, and expands rapidly beyond this point. The trachea is 12 cm long according to Weibel³¹, and 13.5 cm long according to van den Berg²⁹.

Jackson *et al.*¹⁶ suggested that a uniform tube model of the lower airways might be inappropriate, and found that a conical model could explain the deviation of Sg1 without reference to the mechanical impedance of the walls. The suggestion of van den Berg²⁹ that the shape of the expanding area function causes the higher Sg1 frequencies does not appear to have been investigated any further.

Part of the difficulty of resolving the physical cause of the Sg1 deviation has been the lack of subglottal resonance (SGR) measurements from significant numbers of speakers. Van den Berg²⁹ reported his basic results based on only a single human cadaver and a single dog cadaver, and Jackson *et al.*¹⁶ measured SGRs in six excised dog lungs. Ishizaka *et al.*¹⁵ measured SGRs in five tracheostomized patients, and Habib *et al.*¹⁰ measured SGRs in nine awake, intubated patients during a bronchoscopic alveolar lavage procedure. More recent investigations of SGRs have focused on the relation between the individual SGRs and the vowel formants in speech, and the deviation of Sg1 has simply been taken for granted^{2,3,18,20,21,23}.

In this paper, we present data from 50 adult native speakers of American English (25 male and 25 female) that we believe resolves the question of Sg1 deviation. Section 2 details the experiment and analysis methods. In Section 3, the experimental data are presented and a uniform tube model of the subglottal airways is discussed. It is shown that the deviation of Sg1 is accounted for

by the effect of yielding walls on the wave propagation velocity.

II. METHODS

A new speech corpus including simultaneous accelerometer recordings of subglottal acoustics was used²². Recordings were made of 25 male and 25 female adult native speakers of American English between the ages of 18 and 25 years in a sound-attenuated booth. The recordings were made with a SHURE PG27 side-address condenser microphone placed roughly 20 cm in front of the speaker's mouth and slightly to one side. Simultaneously, a K&K Sound HotSpot accelerometer placed on the skin of the neck just below the thyroid cartilage was used to record the vibrations of the neck surface, which in this location is closely related to the acoustic pressure variations at the top of the trachea (see below). The sampling rate for both microphone and accelerometer signals was 48 kHz, and the bit rate was 16. Both signals were recorded simultaneously to a Dell XPS computer using an M-Audio MobilePre USB pre-amplifier. The corpus includes two tokens of the sustained vowel [a:] produced by each speaker, in which there was special emphasis on obtaining high quality accelerometer recordings with clear resonance structure up to the third resonance (Sg3). These recordings were analyzed for the present study. The self-reported height of each participant was also recorded in feet and inches and later converted into centimeters, in order to estimate the length scale of the subglottal airways for each speaker. The error in these height values is therefore estimated to be of the order of a few centimeters.

Accelerometer signals from the skin of the neck below the thyroid cartilage are closely related to the subglottal input impedance, since the phonation source is primarily a volume velocity source and it is the pressure fluctuations just below the glottis that cause the tracheal walls and surrounding tissues and skin to vibrate. The difference between the accelerometer signal and the subglottal input impedance lies principally with the possibility of acoustic coupling between the subglottal airways and the vocal tract during phonation. Any such coupling affects the pressure fluctuations in the trachea and hence also the accelerometer signal, whereas the subglottal input impedance by definition does not include such effects. It has been shown that when a vocal tract formant is close to a subglottal resonance, coupling is relatively large and may result in observable effects on the speech acoustic (microphone) spectrum²⁷. On the other hand, when the formants and subglottal resonances are not particularly close together, the effects of coupling are relatively small and can in fact be neglected, to a first approximation. On average, the first three resonances of the subglottal airways have been reported in the vicinity of 600 Hz, 1400 Hz, and 2100 Hz for adult males, and somewhat higher frequencies for adult females. In contrast, the first three formants in the vowel [a:] are typically in the vicinity of 800 Hz, 1100 Hz, and 2500 Hz for adult males, and somewhat higher frequencies for adult females. Measurement

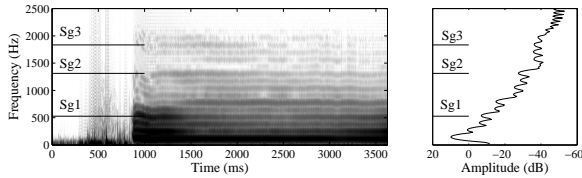


FIG. 2. *Left*: Spectrogram of the accelerometer signal during sustained production of the vowel [a:]. *Right*: DFT spectrum computed using a moderately long window (encompassing several pitch periods) and averaged over the entire utterance so that individual harmonics are resolved. The short horizontal lines labeled ‘Sg1’, ‘Sg2’, and ‘Sg3’ in both panels show the values of the estimated SGR frequencies. The additional small peak between Sg1 and Sg2 is likely due to F1.

of SGRs from the accelerometer signal during a sustained vowel [a:] should therefore result in frequencies close to those of the subglottal input impedance resonances.

Accelerometer signals were down-sampled to 5000 Hz before analysis. A sample spectrogram and average spectrum from one such accelerometer signal is shown in Figure 2. Measurements of Sg1, Sg2, and Sg3 were made by visual inspection of the resonance peaks in the accelerometer spectrogram, averaged DFT spectrum, and LPC spectrum for both [a:] tokens from each of the 50 speakers. Whenever the determination of a resonance peak could be made with confidence, it was recorded. In some cases the signal was not of sufficient quality to identify Sg3, since the tissues and skin act as a low-pass filter with a cutoff frequency which could not always be kept above Sg3. In these cases, the frequency of Sg3 was simply left blank. Similarly, in cases where Sg1 or Sg2 could not be identified with confidence, they were also left blank. It is particularly worth noting that identification of Sg1 is often difficult, given that acoustic coupling effects are greater at lower frequencies, and therefore the Sg1 spectral peak can merge to some degree with another spectral peak related to F1. Sg1 can also have a relatively low amplitude^{12,14,15}, making it hard to distinguish among the lowest source harmonics both in DFT and LPC spectra (in the example of Figure 2, Sg1 is barely visible between the 3rd and 5th harmonics). In spite of these difficulties, all three SGRs could confidently be identified in the majority of cases: of the 100 possible measurements of each SGR, Sg1 was measured 89 times, Sg2 was measured 99 times, and Sg3 was measured 87 times. For three speakers out of 50, Sg1 was not measured in either recording, and for three different speakers, Sg3 was not measured in either recording. For the remaining 44 speakers, at least one measurement was made for each of the three SGRs. The reliability of these measurements was tested by plotting the measured SGR frequencies measured from the accelerometer signal of one [a:] token against those measured from the other token. The result indicated reasonably good agreement between the pairs of measurements, as shown in Figure 3 (r -values for Sg1, Sg2, and Sg3 are 0.60, 0.79, and 0.78, respectively).

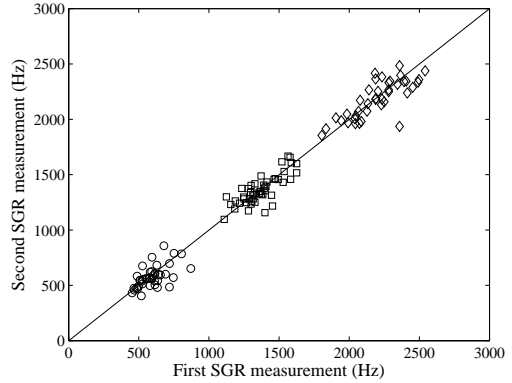


FIG. 3. Reliability of the SGR measurements made in this study. Measurement of SGRs in two different tokens of the sustained vowel [a:] per speaker are plotted against each other, showing good agreement. Sg1: (○); Sg2: (□); Sg3: (◇).

III. RESULTS AND DISCUSSION

The measured frequencies of Sg1 (○), Sg2 (□), and Sg3 (◇) are plotted against participant height in Figure 4. On the assumption that Sg2 and Sg3 are resonances of a uniform, rigid-walled tube with length proportional to the height of the participant, a scaling factor was determined which led to the best fit of Sg2 and Sg3 together using the equation:

$$SgN = \frac{(2N - 1)c_0}{4 \cdot h/k_a} \quad (1)$$

where N is the resonance number, $c_0 = 359$ m/s is the free-field speed of sound in saturated air at body temperature, h is the participant height in meters, and $k_a = 8.508$ is the scaling factor which was found to produce the best fit to all of the Sg2 and Sg3 data (99 Sg2 measurements plus 87 Sg3 measurements; the root-mean-squared error was $\mathcal{E}_{rms} = 32$ Hz). The resulting model predictions are plotted in Figure 4 as solid lines for Sg2 and Sg3, as well as for Sg1 using the same equation. [When males and females are considered separately, the values of k_a are found to be 8.422 and 8.577, with root-mean-squared errors of 28 Hz and 35 Hz, respectively.] It is apparent that the Sg1 measurements are significantly higher in frequency than the model predictions ($\mathcal{E}_{rms} = 168$ Hz), as expected based on the previous studies outlined in Section I.

A. Uniform tube model of subglottal airways

Before turning to an explication of Sg1 deviation, it is worth digressing to investigate the origin of the value of the scaling factor, $k_a = 8.508$. If it is truly appropriate to model the subglottal airways as a rigid-walled, uniform tube, the length of such a tube would be given by $L_a = h/k_a$. Let this be the ‘acoustic length’ of the

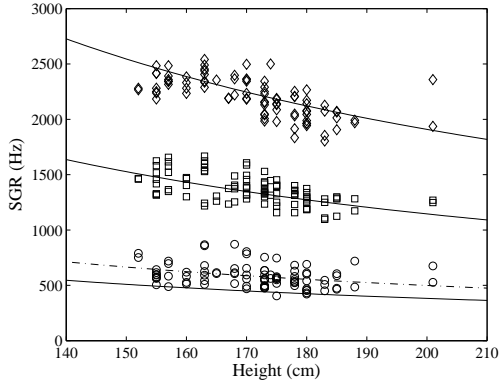


FIG. 4. Measured SGR frequencies vs. self-reported height. Sg1: (○); Sg2: (□); Sg3: (◇). Model predictions are plotted as solid lines for all three SGRs under the assumption of rigid walls. A corrected model prediction for Sg1 based on a change in the wave propagation velocity due to soft-wall resonance is plotted as a dashed line, as described in Section III.B.

subglottal airways, and k_a be the ‘acoustic scaling factor’. Ishizaka *et al.*¹⁵, Gupta *et al.*⁹, and Chi and Sonderegger² found the ‘acoustic length’ to be $L_a \approx 20$ cm, while Flanagan⁴ assumed $L_a \approx 15$ cm (not 17 cm, as reported by Ishizaka *et al.*¹⁵), and van den Berg²⁹ assumed $L_a \approx 26$ cm. A histogram of the values $L_a = h/k_a$ found for the 50 participants in this study is shown in Figure 5, along with histograms and model predictions of the ratios $Sg2/Sg1$, $Sg3/Sg1$, and $Sg3/Sg2$. The distribution of L_a is nearly Gaussian with a peak in the vicinity of $L_a = 20$ cm. A histogram of previously reported data^{10,18} shows a similar peak near $L_a = 20$ cm (data not shown).

As mentioned in Section I, the area function of the subglottal airways as determined from anatomical measurements of airway lengths and diameters^{26,31} has been shown to be roughly constant down to about 20 cm below the glottis, beyond which the area increases dramatically^{15,29} (see Figure 1). Of this 20 cm length, roughly 60% is comprised of the trachea alone, and this ratio appears to be constant across age, height, and gender^{6,24}. Since measurements of trachea length have been reported in both adults and children as a function of height, we may use these data to further test whether the scaling factor $k_a = 8.508$ is anatomically meaningful. Specifically, we may test the prediction that the ratio of height, h , to trachea length, L_t , is equal to a ‘trachea scaling factor’, k_t , defined as $k_t = h/L_t = k_a/0.6$.

Trachea length and height data published by Griscom and Wohl⁵ and Griscom *et al.*⁷ were estimated by applying the program *Tracer*, v.1.7¹⁹ to the published figures of trachea length vs. height. Similar data from Butz¹ were read from a table. The trachea length, L_t , is shown plotted vs. height, h , in Figure 6, with a diagonal line giving the predicted trachea length from the relation $L_t = h/k_t$, where $k_t = k_a/0.6 = 14.1800$. The predicted value of k_t is very close to the reciprocal of the slope of the best fit line passing through the origin,

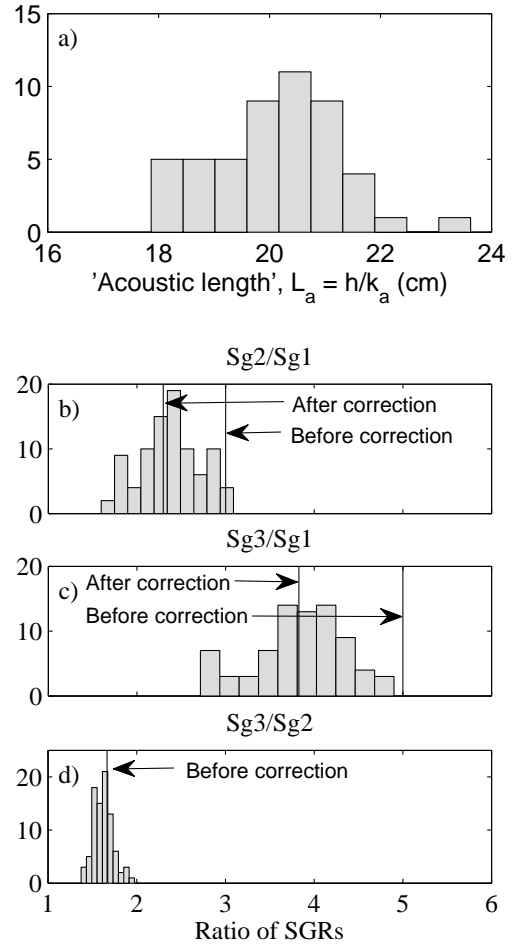


FIG. 5. a): Histogram of h/k_a , corresponding to the ‘acoustic length’ of the subglottal airways. The distribution is nearly Gaussian with a peak near 20 cm. b-d) (from top to bottom): Histograms of the ratios $Sg2/Sg1$, $Sg3/Sg1$, and $Sg3/Sg2$. Vertical lines indicated by arrows represent the predicted values for a uniform tube with rigid walls both before and after correcting for the frequency-dependent wave propagation velocity, as described in Section III.B. Without this correction, only $Sg3/Sg2$ is accurately predicted by such a model.

which is $1/14.0206$. We may therefore conclude that a rigid-walled, uniform tube with a length equal to about $1/k_a$ times the height of any given speaker is an anatomically appropriate model for estimating the frequencies of Sg2 and Sg3. The rapid expansion of the area function beyond 20 cm below the glottis essentially acts as an infinite plane baffle, so that the tube can be considered open at this distal end^{14,15,17,21}.

B. Sg1 deviation and wave propagation velocity

We now return to the question of Sg1 deviation. Given that a simple tube model of the subglottal airways is appropriate for determining the frequencies of Sg2 and Sg3, why is the model prediction of Sg1 frequency signif-

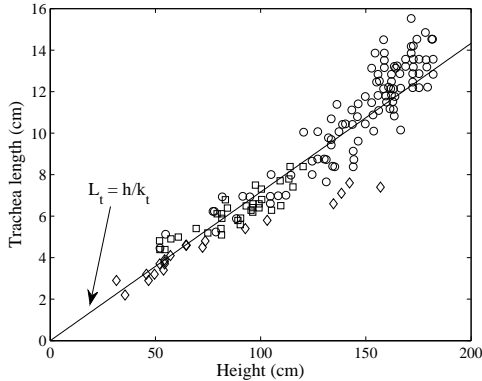


FIG. 6. Trachea length vs. height, spanning the range from newborn to 20 years of age. The data points were gleaned from Griscom and Wohl⁵ (\circ), Griscom *et al.*⁷ (\square), and Butz¹ (\diamond). The diagonal line indicates the relation predicted by $L_t = h/k_t$, and has a root-mean-square error of $\mathcal{E}_{rms} = 1.2$ cm, whereas a linear regression results in a root-mean-square error of $\mathcal{E}_{rms} = 1.1$ cm.

icantly lower than actual measurements? As indicated in Section I, one possibility is that the wave propagation velocity differs from $c_0 = 359$ m/s in the subglottal airways at low frequencies. Since Sg1 measurements are higher than predicted by the tube model, this would require the wave propagation velocity to be *greater than* c_0 in the frequency range of Sg1.

It is known that the speed of pulse waves in compliant-walled tubes, such as arterial blood vessels, is reduced when compared to the speed of the same pulse waves in rigid-walled tubes²⁸. As previously mentioned, van den Berg²⁹ assumed that the subglottal airway walls were compliant in just this way, leading to a reduced wave propagation velocity and a low Sg1 frequency in the vicinity of 300 Hz. Ishizaka *et al.*¹⁵, however, claimed that the airway walls are inertive rather than compliant. In reality, the airway walls have a compliant as well as an inertive component, as both van den Berg²⁹ and Ishizaka *et al.*¹⁵ were aware, and they may therefore resonate at a specific frequency⁸. Moreover, since the airway walls are comprised of two types of tissue (alternating soft tissue and cartilage), each with different compliance and inertance properties, there may in fact be two separate resonance frequencies for the airway walls^{10,28}. At frequencies below the first wall resonance, the walls are compliant, and the wave propagation velocity is lower than c_0 . At frequencies above the second wall resonance, the walls are inertive, and the wave propagation velocity is higher than c_0 . At significantly higher frequencies, the walls begin to behave as if they were rigid, and the wave propagation velocity approaches c_0 . At frequencies between the first and second wall resonances, the wall behavior is more complex, as is the wave propagation velocity as a function of frequency.

Suki *et al.*²⁸ measured the wave propagation velocity and input impedance in calf tracheae and found resonance peaks associated with the soft tissue and cartilage

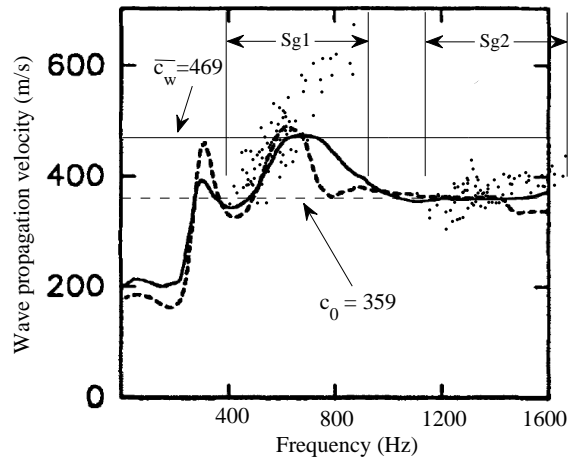


FIG. 7. Wave propagation velocity vs. frequency in one of the calf tracheae measured by Suki *et al.*²⁸. Their figure has been adapted to indicate both the free-field speed of sound, c_0 (horizontal dashed line), and the average wave propagation velocity in the vicinity of Sg1, \bar{c}_w (horizontal solid line). The frequency-dependent solid and dashed lines indicate the wave propagation velocity measured in the stretched and unstretched calf tracheae. Data points indicate the wave propagation velocity, c_w , calculated from human SGR measurements as described in Section III.C. The ranges of Sg1 and Sg2 frequencies are also indicated.

of the trachea walls at ~ 350 Hz and ~ 650 Hz (see Figure 7). Below the first resonance the wave propagation velocity drops rapidly until it reaches a value around 200 m/s or less. This explains the low wave propagation velocity obtained by van den Berg²⁹, who made his measurements in the range from 90 Hz to 300 Hz.

We assumed that the wall properties of calf and human tracheae are roughly similar^{10,28}, and estimated that the average wave propagation velocity in the frequency range normally occupied by Sg1 (~ 600 Hz) is $\bar{c}_w \approx 469$ m/s, as shown in Figure 7. The wave propagation velocity in the frequency range of Sg2 and Sg3 is apparently close to the free-field speed of sound, $c_0 = 359$ m/s, consistent with our analysis thus far (note, however, that Suki *et al.*²⁸ assumed a value of $c_0 = 340$ m/s based on their experimental conditions). When the frequencies of Sg1 predicted by the rigid-walled, uniform tube model are multiplied by $\bar{c}_w/c_0 = 469/359$ to correct for the effect of non-rigid wall resonance on the wave propagation velocity (shown by the dotted line in Figure 4), the observed Sg1 deviation is well accounted for by the resulting corrected model:

$$Sg1' = Sg1 \frac{\bar{c}_w}{c_0} = \frac{\bar{c}_w}{4 \cdot h/k_a} \quad (2)$$

This model of $Sg1'$ results in a fit of the Sg1 data with a root-mean-squared error $\mathcal{E}_{rms} = 96.33$ Hz [the best-fit root-mean-squared error differs by less than 0.001 Hz.]. In addition, the predicted ratios $Sg2/Sg1 = 3$ and

$Sg3/Sg1 = 5$ can be corrected by multiplying them by $c_0/\bar{c}_w = 359/469$. These corrected ratios are shown in panels b) and c) of Figure 5, and they are clearly near the centers of their respective distributions.

C. Individual variability

The results so far have shown that Sg1 deviation can be accounted for *on average* by an increased wave propagation velocity, $\bar{c}_w = 469$ m/s. In order to further test the appropriateness of this model on an individual basis, the frequency dependent wave propagation velocity was calculated for each subject according to the following equation derived by combining Equations 1 and 2:

$$c_w(SgM) = \left[\frac{(2N-1)c_0}{SgN} \right] \cdot \left[\frac{SgM}{2M-1} \right] \quad (3)$$

To calculate $c_w(Sg1)$ (i.e. the wave propagation velocity at the frequency of Sg1), we let $M = 1$ and $N = 2$ (M and N refer to the M^{th} and N^{th} resonances, respectively). For the calculation of $c_w(Sg1)$, it was explicitly assumed that the wave propagation velocity in the frequency range of Sg2 is equal to the free-field speed of sound, $c_w(Sg2) = c_0$, consistent with the results from calf tracheae (see Figure 7). We also calculated $c_w(Sg2)$ (i.e. no longer assuming that $c_w(Sg2) = c_0$) by setting $M = 2$ and $N = 3$ and assuming $c_w(Sg3) = c_0$. The resulting values of $c_w(Sg1)$ and $c_w(Sg2)$ are superimposed on the calf trachea wave propagation velocity data in Figure 7. Except for the highest Sg1 frequencies, the calculated propagation velocities agree surprisingly well with the calf trachea data. Figure 8 shows that the wave propagation velocity at the frequency of Sg1, $c_w(Sg1)$, calculated from Sg2 agrees well with the wave propagation velocity calculated from Sg3. This agreement indicates that the wave propagation velocity in the frequency range of the higher resonances (Sg2 and Sg3) is indeed approximately constant and equal to the free-field speed of sound.

Values of $c_w(Sg1)$ computed from the first [a:] token across speakers were correlated with values computed from the second token ($r = 0.55$). This correlation was similar to the correlation between Sg1 measurements as shown in Figure 3, indicating satisfactory within-speaker reliability. There was no significant difference in $c_w(Sg1)$ between male and female speakers [two-sample t-test; $p = 0.6070$], and no correlation between $c_w(Sg1)$ and speaker height [r -values for height vs. $c_w(Sg1)$ were 0.0499 for males, -0.0820 for females, and 0.0346 for males and females combined].

Gender dimorphisms in subglottal anatomy appear to be functions only of height. For example, Griscom and Wohl⁶ showed that there is no significant difference between male and female trachea lengths until at least 18 years of age. At 20 years, the ratio between the mean male trachea length and the mean female trachea length appears to be approximately $13/11.75 \approx 1.1064$ (see their Figure 1). For the speakers in our study, the ratio of

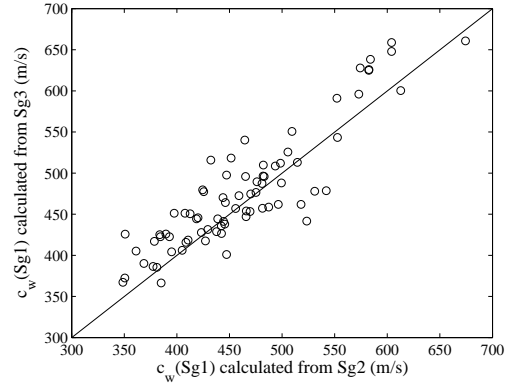


FIG. 8. Wave propagation velocity at Sg1 frequencies calculated from Equation 3 using Sg2 vs. wave propagation velocity calculated using Sg3. The two sets of values agree well ($r = 0.89$).

mean male height to mean female height is 1.0905, which is essentially the same as the ratio for trachea lengths.

The agreement between the calculated wave propagation velocities and the data of Suki *et al.*²⁸ (Figure 7) suggests that the mechanical properties of the calf trachea walls are roughly similar to those of the human airway walls up to ~ 20 cm below the glottis (i.e. the ‘acoustic length’ of the subglottal airways), consistent with our assumption in Section III.B.

It is worth noting that Habib *et al.*¹⁰, using an inverse model of the subglottal airways to estimate wall mechanical properties in humans based on measured subglottal input impedances, and assuming similar tissue densities in humans and calves, obtained values of the soft tissue coefficient of viscosity in humans similar to what was reported for calves in their earlier study²⁸. They obtained Young’s modulus values, Y , which were significantly smaller in humans than those of the calf trachea. However, the wave propagation velocities calculated using their Sg1 and Sg2 values¹⁰ and Equation 3 agree with the data in Figure 7 (data not shown). It is possible that the (reasonable) model simplifications they introduced in order to make the inversion problem tractable may have led to estimates of Y in humans which are physiologically reasonable but ultimately inaccurate, or, as they point out, it may be that such discrepancies between studies are the result of different initial stresses on the soft tissues¹⁰. Alternatively, the fact that c_w for the highest Sg1 frequencies departs significantly from the calf data may be reflective of significant differences between calf and human tracheal tissue mechanical properties. It is difficult to resolve this question, however, because the calf data in Figure 7 are from a single trachea, whereas the human data in the present study are comprised of c_w calculations from 50 individuals.

The complex interplay between wall resonances and wave propagation velocity accounts for the discrepancy between the studies of van den Berg²⁹ and Ishizaka *et al.*¹⁵. van den Berg²⁹ determined that the airway walls were compliant after making measurements

of whole-respiratory tract resonances below 300 Hz. If he had measured resonances at higher frequencies, he would have obtained very different results. On the other hand, the claim of Ishizaka *et al.*¹⁵ that the airway walls are simply inertive is not entirely borne out by the data presented here. They assumed that the airway wall resonance was less than 100 Hz. If this were true, then the calculated wave propagation velocity, c_w , should monotonically decrease to approach the free-field speed of sound, c_0 , as a function of Sg1 frequencies. Our data show the opposite trend: c_w increases as a function of Sg1 frequency, and for some speakers the value of $c_w(\text{Sg1}) \approx c_0$. Moreover, if the wall resonance was less than 100 Hz, then van den Berg²⁹ likely would have obtained data leading him to conclude that the walls were inertive rather than compliant, since his measurements were carried out at frequencies higher than the putative wall resonance. Based on the data presented in this study, the wall resonance (or resonances) must be in the vicinity of Sg1 and, depending on the exact mechanical properties of the walls, the walls may be more or less inertive in this frequency range.

In a dispersive system with variable wave propagation velocity (such as the subglottal airways appear to be), the attenuation is also variable^{14,28}. According to Figure 3 in Suki *et al.*²⁸, the attenuation is largest in the frequency range of Sg1. This could at least partially account for the observation that the amplitude of Sg1 is frequently less than expected, even less than the amplitude of Sg2^{12,14,15}.

IV. CONCLUSION

On the basis of accelerometer signals recorded during sustained [a:] vowels, and the heights of 50 adult native speakers (25 men, 25 women) of American English, and verified using data previously reported in the literature, we have confirmed that a simple uniform tube model of the subglottal airways is anatomically and acoustically appropriate for describing subglottal resonances^{15,29}. The main novel findings of this study are: 1) whereas the walls may be considered rigid in the frequency range of Sg2 and Sg3, they must be considered yielding and resonant in the frequency range of Sg1, with a resulting increase in wave propagation velocity which successfully accounts for the deviation of Sg1; 2) the acoustic length of the uniform tube, L_a , varies between approximately 18 cm and 23.5 cm, and is approximately equal to the height of the speaker, h , divided by a scaling factor, $k_a = 8.508$; 3) trachea length can also be predicted from height as $L_t \approx h/k_t$, where $k_t = k_a/0.6 = 14.1800$; and 4) differences in subglottal resonance frequencies between males and females can be accounted for by height-related differences.

Sg2 and Sg3 can be accurately predicted from height if the wave propagation velocity is assumed to be equal to the free-field speed of sound in saturated air at body temperature, $c_0 = 359$ m/s. Prediction of Sg1 depends on a higher wave propagation velocity, $\bar{c}_w \approx c_0 \cdot 469/359$, or $\bar{c}_w \approx \frac{4}{3}c_0$, on average. In arriving at this latter con-

clusion, we have assumed that the mechanical properties (and hence the resonances) of the tracheal walls in calves are similar to those of the large subglottal airway walls in humans down to at least 20 cm below the glottis. This assumption appears to be supported by the fact that wave propagation velocities calculated from measured SGRs using Equation 3 agree well with the calf trachea data. It should be noted that these results were obtained from accelerometer recordings made on adult speakers who are at least 18 years old and who have attained their full height.

In the analysis of speech (microphone) signals, it is sometimes desirable to know the frequencies of the SGRs, especially Sg1 and Sg2^{21,30}, but it can be difficult to measure them. If either of them can be measured in a given portion of the signal, a good estimate of the other can now be obtained using the simple tube model described here and with an appropriate value for the wave propagation velocity. Conversely, if Sg1 and Sg2 can both be measured, either from a microphone or accelerometer signal, the ratio between them may be considered to be related to the resonance frequencies of the airway walls. This relationship may be useful for estimating airway wall mechanical properties²⁸ from non-invasive speech recordings.

Acknowledgments

This work was supported in part by NSF grant No. 0905250.

- ¹ R. O. Butz, "Length and cross-section growth patterns in the human trachea," *Pediatrics*, 336–341 (1968).
- ² X. Chi and M. Sonderegger, "Subglottal coupling and its influence on vowel formants," *The Journal of the Acoustical Society of America* **122**, 1735–1745 (2007).
- ³ T. G. Csapó, Z. Bárkányi, T. E. Gráczy, T. Böhm, and S. M. Lulich, "Relation of formants and subglottal resonances in hungarian vowels," *Proceedings of Interspeech*, 484–487 (2009).
- ⁴ J. L. Flanagan, "Some properties of the glottal sound source," *Journal of Speech Hearing Research* **1**, 99–116 (1958).
- ⁵ N. T. Griscom and M. E. B. Wohl, "Dimensions of the growing trachea related to body height: Length, antero-posterior and transverse diameters, cross-sectional area, and volume in subjects younger than 20 years of age," *American Review of Respiratory Disease*, 840–844 (1985).
- ⁶ N. T. Griscom, M. E. B. Wohl, "Dimensions of the growing trachea related to age and gender," *American Journal of Roentgenology*, 233–237 (1986).
- ⁷ N. T. Griscom, M. E. B. Wohl, and T. Fenton, "Dimensions of the trachea to age 6 years related to height," *Pediatric Pulmonology*, 186–190 (1989).
- ⁸ R. W. Guelke and A. E. Bunn, "Transmission line theory applied to sound wave propagation in tubes with compliant walls," *Acustica* **48**, 101–106 (1981).
- ⁹ V. Gupta, T. A. Wilson, and G. S. Beavers, "A model for vocal cord excitation," *Journal of the Acoustical Society of America* **54**, 1607–1617 (1973).
- ¹⁰ R. H. Habib, R. B. Chalker, B. Suki, and A. C. Jackson, "Airway geometry and wall mechanical properties

- estimated from subglottal input impedance in humans,” *Journal of Applied Physiology* **77**, 441–451 (1994).
- 11 V. P. Harper, S. S. Kraman, H. Pasterkamp, and G. R. Wodicka, “An acoustic model of the respiratory tract,” *IEEE Transactions on Biomedical Engineering* **48**, 543–550 (2001).
 - 12 J. C. Ho and M. Zañartu and G. R. Wodicka, “An anatomically-based, time-domain acoustic model of the subglottal system for speech production,” *The Journal of the Acoustical Society of America* **129**, 1531–1547 (2011).
 - 13 K. Horsfield and G. Dart and D. E. Olson and G. F. Filly and G. Cumming, “Models of the human bronchial tree,” *Journal of Applied Physiology* **31**, 207–217 (1971).
 - 14 H. Hudde and H. Slatky, “The acoustical input impedance of excised human lungs—measurements and model matching,” *The Journal of the Acoustical Society of America* **86**, 475–492 (1989).
 - 15 K. Ishizaka, M. Matsudaira, and T. Kaneko, “Input acoustic-impedance measurement of the subglottal system,” *The Journal of the Acoustical Society of America* **60**, 190–197 (1976).
 - 16 A. C. Jackson, J. P. Butler, and R. W. Pyle, Jr., “Acoustic input impedance of excised dog lungs,” *Journal of the Acoustical Society of America* **64**, 1020–1026 (1978).
 - 17 A. C. Jackson, B. Suki, M. Ucar, and R. H. Habib, “Branching airway network models for analyzing high-frequency lung input impedance,” *Journal of Applied Physiology* **75**, 217–227 (1993).
 - 18 Y. Jung, “Acoustic articulatory evidence for quantal vowel categories: the features [low] and [back],” Ph.D. thesis, MIT (2009), pp. 1–142.
 - 19 M. Karolewski, “Tracer, v. 1.7,” URL <http://sites.google.com/site/kalypsosimulation/Home/data-analysis-software-1> (date last viewed 9/13/10) (2003).
 - 20 S. M. Lulich, “The role of lower airway resonances in defining vowel feature contrasts,” Ph.D. thesis, MIT (2006), pp. 1–145.
 - 21 S. M. Lulich, “Subglottal resonances and distinctive features,” *Journal of Phonetics* **38**, 20–32 (2010).
 - 22 S. M. Lulich, J. R. Morton, M. S. Sommers, H. Arsikere, and A. Alwan, “A new speech corpus for studying subglottal acoustics in speech production, perception, and technology,” *Journal of the Acoustical Society of America* **128**, 2288 (2010).
 - 23 A. Madsack, S. M. Lulich, W. Wokurek, and G. Dogil, “Subglottal resonances and vowel formant variability: A case study of High German monophthongs and Swabian diphthongs,” *Proceedings of LabPhon11*, 91–92 (2008).
 - 24 P. J. F. M. Merkus, A. A. W. ten Have-Opbroek, and P. H. Quanjer, “Human lung growth: A review,” *Pediatric Pulmonology* **21**, 383–397 (1996).
 - 25 W. W. Nichols, M. F. O’Rourke, C. Vlachopoulos, *MacDonald’s Blood Flow in Arteries: Theoretical, Experimental and Clinical Principles* (Hodder Arnold, London, 2005), pp. 64–65.
 - 26 F. Rohrer, “Der Strömungswiderstand in den menschlichen Atemwegen und der Einfluss der unregelmässigen Verzweigung des Bronchialsystems auf den Atmungsverlauf in verschiedenen Lungbezirken,” *Pflügers Archiv* **162**, 225–299 (1915).
 - 27 K. N. Stevens, *Acoustic Phonetics* (MIT Press, Cambridge, MA, 1998), pp. 299–303.
 - 28 B. Suki, R. H. Habib, and A. C. Jackson, “Wave propagation, input impedance, and wall mechanics of the calf trachea from 16 to 1,600 Hz,” *Journal of Applied Physiology* **75**, 2755–2766 (1993).
 - 29 J. van den Berg, “An electrical analogue of the trachea, lungs and tissues,” *Acta Physiol. Pharmacol. Neerlandica* **9**, 361–385 (1960).
 - 30 S. Wang, S. M. Lulich, and A. Alwan, “Automatic detection of the second subglottal resonance and its application to speaker normalization,” *Journal of the Acoustical Society of America* **126**, 3268–3277 (2009).
 - 31 E. R. Weibel, *Morphometry of the Human Lung* (Springer, Berlin 1963), pp. 110–142.
 - 32 M. Zañartu, L. Mongeau, and G. R. Wodicka, “Influence of acoustic loading on an effective single mass model of the vocal folds,” *Journal of the Acoustical Society of America* **121**, 1119–1129 (2007).